Polyhedron 28 (2009) 1057–1064

Contents lists available at ScienceDirect

Polyhedron

journal homepage: www.elsevier.com/locate/poly

Stabilization of the *N*-1-substituted cytosinate iminooxo form in dinuclear palladium complexes

Aleksandar Višnjevac [a], Marija Luić [a], Renata Kobetić [b], Dubravka Gembarovski [c], Biserka Žinić [b,*]

[a] Division of Physical Chemistry, Ruđer Bošković Institute, Bijenička 54, 10000 Zagreb, Croatia
[b] Division of Organic Chemistry and Biochemistry, Ruđer Bošković Institute, Bijenička 54, 10000 Zagreb, Croatia
[c] GlaxoSmithKline, Research Centre Zagreb, Prilaz baruna Filipovića 29, 10000 Zagreb, Croatia

ARTICLE INFO

Article history:
Received 29 November 2008
Accepted 13 January 2009
Available online 14 February 2009

Keywords:
Dinuclear palladium complexes
N-1-substituted cytosine
Iminooxo form
X-ray diffraction
Mass spectrometry
NMR spectroscopy

ABSTRACT

The synthesis, as well as chemical and structural characterization, of 1-(*p*-toluenesulfonyl)cytosine (**1**) and its dinuclear complexes of the composition Pd_2(1-TosC$^-$–*N*3,*N*4)$_4$ (**3**) and Pd_2(1-TosC$^-$–*N*3,*N*4)$_2$DMSO$_2$Cl$_2$ (**4**) by means of ESI-MS, IR, ^{1}H NMR and X-ray single crystal analysis are described. Ligand **1** exists in the preferred aminooxo tautomeric form, while both dinuclear complexes reveal the presence of the iminooxo form of the ligand, where 1-TosC$^-$ stands for the anion of the cytosine derivative of **1**, bridging two palladium atoms. Complex **3** has a paddlewheel structure with two square-planar coordination spheres, consisting of four N atoms each, mutually parallel and perpendicular to the inter-palladium vector. Complex **4** is characterized by two mutually parallel square-planar coordination spheres consisting of two nitrogens, sulfur from the solvent molecule and a chloride. A feasible chemical route for the formation of **3** and **4** *via* the kinetically favoured mononuclear complex Pd(1-TosC–*N*3)$_2$Cl$_2$ (**2**) is proposed, based on the IR, ^{1}H NMR, mass spectrometry, elemental analysis and X-ray structure analysis data.

1. Introduction

The relative stability of tautomers of nucleobases is of the highest importance for the structure and function of nucleic acids. Cytosine is a very important nucleobase with respect to the DNA structure; in its protonated form (C^+), it is involved in the formation of $C \cdot C^+$ DNA duplexes [1,2] and $C \cdot G \cdot C^+$ triplexes [3]. The iminooxo tautomer of cytosine is a mutagenic base analogue capable of pairing with adenine [4]. Although three tautomers (Fig. 1) are possible for *N*-1-substituted cytosine, the aminooxo tautomer **I** has been found to be dominant in the solid state, in aqueous and DMSO solutions, as well as in nucleic acids. Its abundance exceeds the iminooxo tautomer **II** by a factor of 10^4–10^5, while the existence of the iminohydroxo tautomer **III** seems to be uncertain [5].

It has been shown in a number of cases that reactions of metal ions with *N*-1-substituted cytosine, containing a large excess of the preferred tautomer **I**, spontaneously lead to the formation of *N*3,*N*4 or *N*4,*N*4 mononuclear Pd**L**$_2$ complexes containing exclusively the iminooxo form of the cytosine base [6,7]. There are, however, few examples of the coexistence of two forms, aminooxo and iminooxo, within the same structure [8]. In addition, very few metal complexes containing the iminooxo form of the cytosine base have been characterized by X-ray crystallography ([6] and the references therein, [9]).

As a part of our program directed toward the synthesis and characterization of biologically active nucleobase derivatives, we have recently described the synthesis and *in vitro* antitumor activity assays of a series of novel *N*-1-sulfonyluracil and *N*-1-sulfonylcytosine derivatives [10,11]. We hereby report on the preparation and structural characterization of two novel dinuclear Pd(II) complexes of 1-(*p*-toluenesulfonyl)cytosine (**1**), containing exclusively the iminooxo form of the ligand anion (1-TosC$^-$).

2. Experimental

2.1. General remarks

Infrared spectra were recorded on a Perkin–Elmer 297 spectrophotometer with the samples prepared as KBr pellets. ^{1}H and ^{13}C NMR spectra were recorded in DMSO–d_6 on Bruker AV 300 and 600 MHz spectrometers using TMS or DMSO–d_6 as the internal standard. Elemental analyses were done on a Perkin–Elmer 2400 Series II CHNS analyzer. The polycrystalline samples were mounted inside a thin-walled glass capillary (internal diameter 0.3 mm) and measured on an Oxford Diffraction Xcalibur Nova R diffractometer with a microfocusing Cu tube. Conductance measurements were carried out at room temperature using a CD 7A Tacussel conductance bridge for 10^{-3} mol dm^{-3} solutions in DMSO.

* Corresponding author. Tel.: +385 1 4561066; fax: +385 1 4680195.
E-mail address: bzinic@irb.hr (B. Žinić).

0277-5387/$ - see front matter © 2009 Elsevier Ltd. All rights reserved.
doi:10.1016/j.poly.2009.01.043

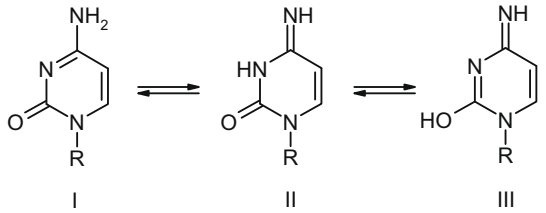

Fig. 1. Tautomers of *N*-1-substituted cytosine.

2.2. ESI-MS

Mass spectral data were acquired on a LCQ Deca ion trap mass spectrometer from ThermoFinnigan (San Jose, CA, USA) equipped with an electrospray ionization (ESI) interface operated in the positive and negative ion modes, mass range 150–2000. Stock samples were prepared in CH_3OH or DMSO, further diluted to a concentration of about 0.05 mg/mL in CH_3CN, CH_3OH or water, and directly injected. Infusion into the mass spectrometer was performed by the built-in syringe pump at a flow rate of 5 μL/min. Nitrogen was used as the auxiliary and sheath gas. Helium was used as the collision gas in the ion trap. The sheath gas flow was set at 85 and the auxiliary gas flow at 30 (arbitrary units). The spray voltage was set at 4.5 kV, while the capillary temperature was 250 °C and the capillary voltage 17 V. Full mass spectra were acquired over the mass range *m/z* 150–2000. Additional solvent cluster studies were performed by varying the capillary voltage (10 V) and temperature (250 °C). For MS/MS investigations, characteristic molecular ions were isolated in the ion trap and collisionally activated with different collision energies (CE) to find the optimal CE for a distinct fragmentation. Product ions in the MS/MS spectra were chosen to perform further MS^3 and MS^4 experiments, relevant to the confirmation of investigated compounds.

2.3. Synthesis

2.3.1. Preparation of ligand *1*

Synthesis of the ligand 1-(*p*-toluenesulfonyl)cytosine (**1**) was performed according to the procedure reported by Kašnar-Šamprec et al. [11]. 1-(*p*-Toluenesulfonyl)cytosine (**1**) had been synthesized previously by the reaction of silylated cytosine and *p*-toluenesulfonyl chloride in acetonitrile, according to Scheme 1. The phenyl-proton (Ph) assignments were confirmed by carbon-proton connectivity in $^1H/^{13}C$ heteronuclear correlation spectra (HETCOR). Additionally, in the NOESY spectrum of **1**, the assignment of Ph-c protons was proved by their interaction with methyl-protons. IR (KBr) ν_{max}/cm^{-1}: 3369 (m), 3100 (m), 3074(m), 1703 (m), 1673 (s), 1524 (s), 1489 (m), 1376 (m), 1353 (m), 1285 (m), 1236 (w), 1184 (m), 1173 (s), 1138 (w), 1116 (m), 1088 (m), 1023 (w), 967 (m), 806 (w), 765 (m), 707 (m), 689 (m), 657 (w), 602 (w), 585 (w), 555 (m), 542 (m); ^1H NMR (DMSO–d_6) δ/ppm: 8.14 (d, 1H, $J_{6,5}$ = 7.8 Hz, H-6), 7.95 (brs, 2H, NH_2), 7.87 (d, 2H, $J_{b,c}$ = 8.1 Hz, Ph-b), 7.46 (d, 2H, $J_{c,b}$ = 8.1 Hz, Ph-c), 5.98 (d, 1H, $J_{5,6}$ = 7.8 Hz, H-5), 2.42 (s, 3H, CH_3); ^{13}C NMR (DMSO–d_6) δ/ppm: 166.27 (s, C-4), 151.22 (s, C-2), 145.61 (s, Ph-d), 139.73 (d, C-6), 134.47 (s, Ph-a), 129.80 (d, Ph-c), 129.02 (d, Ph-b), 97.50 (d, C-5), 21.20 (q, CH_3); MS (EI) exact mass calculated for $C_{11}H_{11}N_3O_3S$: *m/e* 265.051565 ($[M]^+$), found: 265.040053.

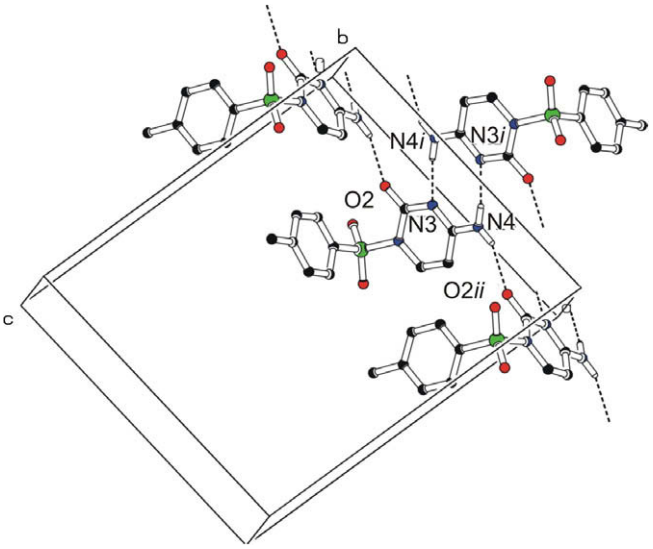

Fig. 2. Packing diagram of **1**.

2.3.2. Preparation of the complex Pd(1-TosC–N3)$_2$Cl$_2$ (*2*)

To a solution of 1-(*p*-toluenesulfonyl)cytosine (**1**) (0.1061 g, 0.4 mmol) in methanol (9 mL), K_2PdCl_4 (0.0653 g, 0.2 mmol) was added. The reaction mixture was stirred and refluxed for 2 h. The red suspension was cooled to room temperature and a pale yellow solid product was filtered off, washed with methanol and dried over vacuo to give 102 mg (76%) of a pale yellow powder **2**: IR (KBr) ν_{max}/cm^{-1}: 3406 (s), 3313 (s), 3288 (s), 3247 (m), 3207 (m), 3107 (m), 3067 (m), 1686 (s), 1650 (s, br), 1613 (s), 1609 (s), 1514 (s), 1503 (s), 1380 (s), 1363 (s), 1276 (s), 1252 (m), 1191 (s), 1171 (s), 1145 (m), 1122 (m), 1107 (m), 1084 (s), 1045 (s), 1017 (m), 974 (m), 815 (m), 792 (s), 766 (s), 706 (s), 695 (s), 673 (s), 613 (s), 590 (s), 552 (s), 541 (s), 480 (m), 361 (m). *Anal.* Calc. for $C_{22}H_{22}Cl_2N_6O_6PdS_2$ xH_2O (M_r = 725.91): C, 36.40; H, 3.33; N, 11.58; S, 8.83. Found: C, 36.05; H, 2.93; N, 11.55; S, 8.54%.

2.3.3. Complex *2* in DMSO-d_6 solution

The first set of signals (marked o in Fig. 4): ^1H NMR (DMSO–d_6) δ/ppm: 8.10 (d, 1H, $J_{6,5}$ = 8.0 Hz, H-6), 7.88 (d, 2H, J = 8.7 Hz, NH_2), 7.84 (d, 2H, $J_{b,c}$ = 8.1 Hz, Ph-b), 7.44 (d, 2H, $J_{c,b}$ = 8.0 Hz, Ph-c), 5.94 (d, 1H, $J_{5,6}$ = 7.9 Hz, H-5), 2.41 (s, 3H, Ph–CH_3); ^{13}C NMR (DMSO–d_6) δ/ppm: 165.90 (s, C-4), 150.87 (s, C-2), 145.28 (s, Ph-d), 139.41 (d, C-6), 134.19 (s, Ph-a,), 129.51 (d, Ph-c), 128.72 (d, Ph-b), 97.25 (d, C-5), 21.11 (q, Ph–CH_3).

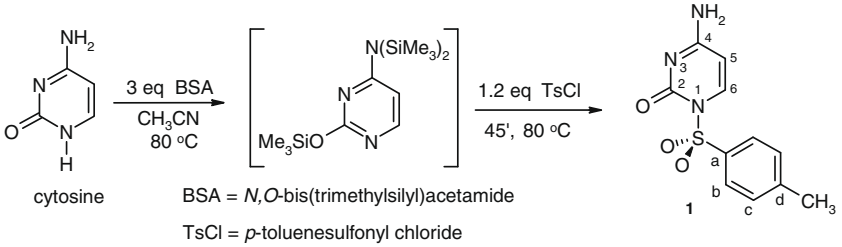

Scheme 1. Synthesis of 1-(*p*-toluenesulfonyl)cytosine (**1**).

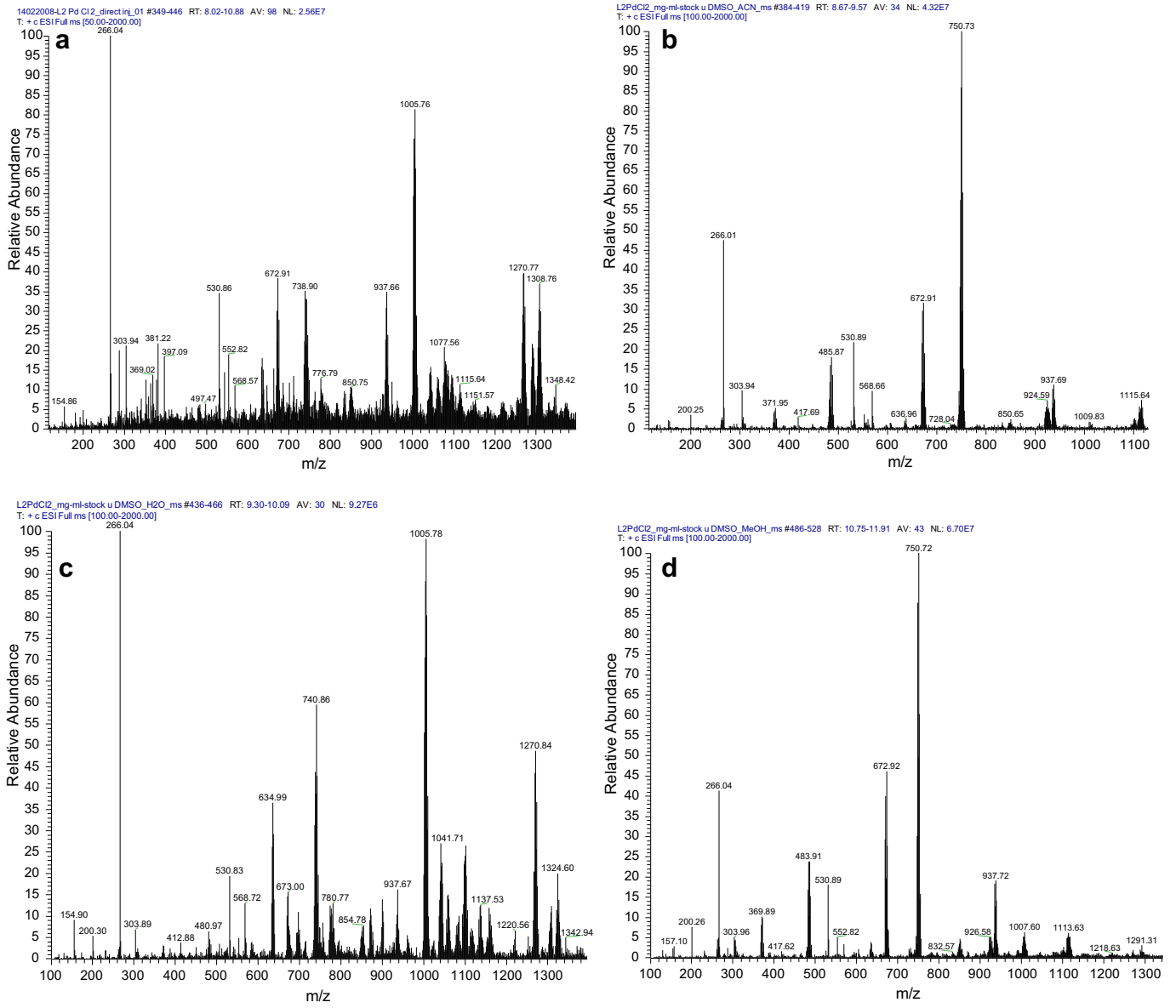

Fig. 3. ESI-MS spectra of the yellow solid Pd**L**$_2$Cl$_2$ (**2**): (a) dissolved in CH_3OH; (b) dissolved in DMSO and diluted with CH_3CN; (c) dissolved in DMSO and diluted with water and (d) dissolved in DMSO and diluted with CH_3OH.

The second set of signals (marked x in Fig. 4): ^{1}H NMR (DMSO–d_6) δ/ppm: 9.34, 9.25, 9.21, 8.89 (4 x brs, 2H, NH), 8.22 (m, 1H, H-6), 7.94 (m, 2H, Ph-b), 7.50 (m, 2H, Ph-c), 6.07 (m, 1H, H-5), 2.43 (s, 3H, Ph–CH_3); ^{13}C NMR (DMSO–d_6) δ/ppm: 163.82 (s, C-4), 148.99 (s, C-2), 146.39 (s, Ph-d), 139.46 (d, C-6), 132.64 (s, Ph-a), 129.92 and 129.77 (d, Ph-c), 129.23 and 129.20 (d, Ph-b), 97.20 (d, C-5), 21.22 (q, Ph–CH_3).

2.3.4. Preparation of complexes *3* and *4*

Slow evaporation of the DMF solution of solid material **2** at room temperature gave, after 10 days, orange needles of complex **3**, whereas a 60-day-long crystallization from the DMSO solution of solid material **2** at room temperature gave crystals of complex **4**. Single crystals of **3** and **4** were characterized by X-ray crystallography.

Complex Pd$_2$(1-TosC$^-$–N3,N4)$_2$DMSO$_2$Cl$_2$ (***4***): IR (KBr) ν_{max}/cm^{-1}: 3407 (w), 3247 (w), 3103 (w), 3012 (w), 2919 (w), 1670 (s), 1648 (s), 1569 (s), 1475 (m), 1396 (m), 1354 (m), 1282 (s), 1236 (m), 1188 (s), 1172 (s), 1148 (s), 1128 (s), 1087 (s), 1043 (s), 1025 (s), 954 (w), 808 (w), 757 (w), 723 (m), 680 (m), 651 (w), 607 (vw), 560 (s), 546 (m), 491 (m), 426 (m), 370 (br, m), 360 (m, sh), 249 (m); ^{1}H NMR (DMSO–d_6) δ/ppm: 7.85 (d, 2H, $J_{b,c}$ = 8.3 Hz, Ph-b), 7.52 (d, 1H, $J_{6,5}$ = 8.0 Hz, H-6), 7.45 (d, 2H, $J_{c,b}$ = 8.2 Hz, Ph-c), 7.26 (brs, 1H, NH-4), 5.92 (d, 1H, $J_{5,6}$ = 8.0 Hz, H-5), 2.93 (s, 3H $(CH_3)_2SO$–Pd), 2.54 (s, 3H $(CH_3)_2SO$–Pd), 2.42 (s, 3H, Ph–CH_3).

2.4. X-ray structural analysis

Crystal data, data collection and refinement parameters for compounds **1**, **3** and **4** are summarized in Table 1. Data collections were performed on an Enraf Nonius CAD4 diffractometer using graphite monochromated Cu Kα radiation (λ = 1.54179 Å). Data reduction and cell refinement were carried out using the procedures incorporated into the WINGX package [12]. Intensities were measured at room temperature. All structures were solved using direct methods with SIR2002 [13] and refined using the full matrix least-squares refinement based on F^2 with SHELXL [14]. Molecular illustrations were prepared using ORTEP-III [15]. All non-hydrogen

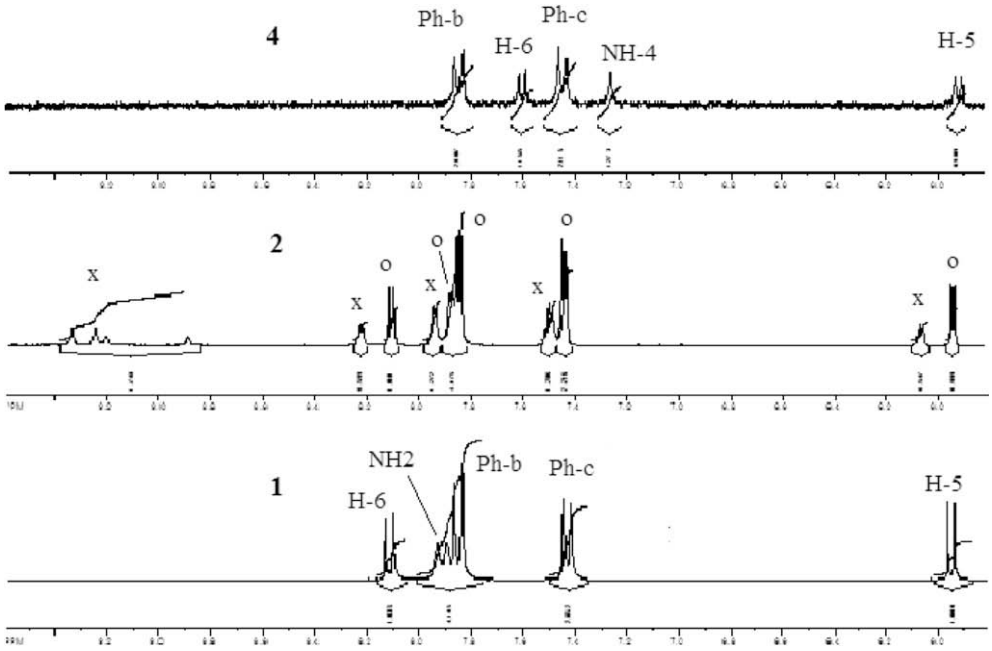

Fig. 4. (DMSO–d_6) ^{1}H NMR spectra of ligand **1** (bottom), complex Pd**L**$_2$Cl$_2$ (**2**) at room temperature (middle) and complex Pd$_2$(1-TosC$^-$–*N*3,*N*4)$_2$DMSO$_2$Cl$_2$ (**4**) (top).

atoms in the structures were refined anisotropically; hydrogen atoms were included in their geometrically calculated positions (except for some hydrogen atoms included in hydrogen bonding) and refined according to the riding model. In the structure of **3**, the substantial residual electron density due to the unresolvable disorder of solvent molecules was reduced by the SQUEEZE [16] routine incorporated into PLATON [17].

3. Results and discussion

3.1. Synthesis and crystal structure of ligand *1*

The synthesis of the ligand 1-(*p*-toluenesulfonyl)cytosine (**1**), (1-TosC), was performed according to the procedure reported by Kašnar-Šamprec et al. [11]. Silylation of cytosine was accomplished with *N*,*O*-bis(trimethylsilyl)acetamide in acetonitrile at 80 °C. Condensation of silylated cytosine with *p*-toluenesulfonyl chloride in acetonitrile gave ligand **1** in 80% yield after recrystallization from methanol (Scheme 1).

In our previous report, we have shown that *N*-1-sulfonyluracil derivatives can adopt chiral conformations, possessing *M* and *P* helicities in the crystalline state [18]. A partial and a total spontaneous resolution upon crystallization was observed for 1-(*p*-toluenesulfonyl)uracil and 1-(1-naphthylsulfonyl)uracil, respectively, while the structurally closely related 1-(*p*-toluenesulfonyl)thymine crystallized as a racemic compound. Unlike its uracil counterpart, 1-tosylcytosine (ligand **1**) does not exhibit *à la Pasteur* separation of conformational enantiomers upon crystallization,

Table 1
Crystallographic data for compounds **1**, **3** and **4**.

Compound	**1**	**3** (squeezed)	**4**
Formula	$C_{11}H_{11}N_3O_3S$	$C_{44}H_{36}N_{12}O_{12}Pd_2S_4$	$C_{30}H_{44}Cl_2N_6O_{10}Pd_2S_6$
Formula weight (g mol^{-1})	265.00	1269.92	1124.77
Crystal color and habit	colorless plate	yellow needle	yellow plate
Crystal dimensions (mm)	0.25 × 0.20 × 0.07	0.3 × 0.07 × 0.07	0.2 × 0.15 × 0.05
Crystal system	monoclinic	orthorhombic	monoclinic
Space group	$P2_1/c$	*Pnab*	*C*2/*n*
a (Å)	13.166 (2)	17.372(3)	42.122(8)
b (Å)	5.660 (3)	17.882(2)	12.5940(9)
c (Å)	15.95 (1)	21.570(5)	16.6390(7)
β (°)	96.02 (5)	90.	97.12(4)
V (Å^3)	1182 (1)	6701(2)	8759(2)
Z	4	4	8
ρ_{calc} (g cm^{-1})	1.491	1.295	1.706
μ (Cu Kα) (mm^{-1})	2.503	5.969	10.915
Absorption correction	none	ψ-scan	ψ-scan
F(000)	552	2560	4544
θ max. (°)	76.46	76.07	76.4
No. of reflections collected	3126	6976	9308
No. of reflections observed [$I > 2\sigma(I)$]	1966	1607	6889
Parameters	120	337	515
R_1	0.0444	0.0777	0.0915
wR_2	0.1234	0.2320	0.2717
ρ_{max}, ρ_{min} (e Å^{-3})	0.71, −0.58	1.13, −1.80	2.62, −2.32

and crystallizes in the centrosymmetric space group $P2_1/a$. However, it exhibits analogous conformational chirality in the solid state with respect to the S–N bond. This is due to the enhanced hydrogen bonding potential of the cytosine, where the presence of a double hydrogen bond donor (amino nitrogen N4) instead of a single H bond donor (endocyclic N3–H) in the case of the uracil derivative, enables the formation of centrosymmetric dimers and tetramers, and finally leads to a centrosymmetric crystal arrangement. The crystal structure of the ligand **1** is characterized by hydrogen-bonded centrosymmetric dimers of the graph set motif $R_2^2(8)$ [19], formed by hydrogen bonds N4–H4b···N3*i*, and centrosymmetric tetramers of the graph set motif R_4^4 including hydrogen bonds N4–H4b···N3*i* and N4–H4a···O2*ii* (Fig. 2). Thus, these two hydrogen-bonded centrosymmetric rings share the common edge made by the hydrogen bond N4–H4B···N3*i* and form an infinite double layer along the crystallographic *a*-axis.

3.2. Synthesis and characterization of complexes **2**, **3** and **4**

3.2.1. Synthesis

1-(*p*-Toluenesulfonyl)cytosine (**1**) and K_2PdCl_4 in a 2:1 molar ratio were refluxed for 2 h in methanol and, upon cooling to room temperature, the pale yellow solid **2** was obtained. Solid **2** is soluble in polar coordinative solvents like DMF and DMSO, and insoluble in most other organic solvents and in water. The same solid product **2** was obtained using DMF instead of methanol, as proved by the X-ray powder diffraction method (data not shown). Slow evaporation of a DMF solution of solid material **2** over 10 days at room temperature gave orange needles of complex **3**, whereas a 60 day crystallization of the DMSO solution at room temperature gave crystals of complex **4** (Scheme 2). The structures of complexes **3** and **4** were confirmed by X-ray structural analysis.

The molecular formula of the pale yellow solid **2** ($Pd\mathbf{L}_2Cl_2$, where **L** = 1-(*p*-toluenesulfonyl)cytosine) (**1**) was confirmed by elemental analysis and ESI-MS spectrometry.

3.2.2. ESI-MS studies

Since ESI-MS is the softest desorption/ionization method, it is ideally suited to investigate the coordination behaviour of transition metal complexes [20,21]. The mass spectrum reflects the composition of the species present in the solution. Franska studied cytosine platinum(II) complexes by ESI-MS in DMSO and observed the formation of cationic complexes with Pt(II). Singly charged [cytosine + PtCl + 2DMSO]$^+$ ions were detected at a low cone voltage [22].

Our MS studies (ESI-MS and HRMS) confirmed the molecular formula of complex **2**. The spectra were taken at a low cone voltage (10 V). Molecular ions containing palladium gave rise to a number of peaks showing the characteristic natural isotope percent distribution of the compounds containing one or two palladium atoms. Masses of the complexes reported in this paper are those containing the most abundant stable isotope of each element in the complex. Since the examined solid, complex **2**, had a low solubility in CH_3OH or CH_3CN, these being the common solvents used for ESI-MS studies, it was dissolved in DMSO and then diluted with CH_3OH, water or CH_3CN in our experiments (Fig. 3). The obtained spectra were compared with the theoretical spectra, matching completely the molecular peak percent distribution caused by the Pd isotopes.

The presence of the complex $Pd\mathbf{L}_2Cl_2$ (**2**) was confirmed by detection of the ions from CH_3OH solutions: at *m/z* 635.00 assigned as the [Pd**L**(**L**–H)]$^+$ ion and at *m/z* 672.91 assigned as [Pd$\mathbf{L}_2$Cl]$^+$, or DMSO solutions: at *m/z* 730.78 assigned as the [(Pd$\mathbf{L}_2Cl_2$)Na]$^+$ ion and at *m/z* 748.75 assigned as the [(Pd$\mathbf{L}_2Cl_2$)K]$^+$ ion, in the ES$^+$ mode. The mononuclear complex $Pd\mathbf{L}_2Cl_2$ exchanged chloride quickly with another ligand forming a $Pd\mathbf{L}_3Cl$ type complex. The presence of that complex was confirmed after detection of the ions from CH_3OH solution: at *m/z* 937.75 assigned as the (Pd$\mathbf{L}_3$Cl)$^+$ ion. Dissolving complex **2** in DMSO and further diluting with water, methanol or acetonitrile showed clearly that the species present in the solutions depend strongly on the added solvent properties. The formation and stability of the formed species were monitored by ESI-MS and LC–MS. Interaction between complex **2** and DMSO was detected as a new species eluted at a retention time of 48.67 minutes with *m/z* 1086 and assigned as [Pd$_2\mathbf{L}_3$(DMSO)]$^+$.

It was also found that when complex $Pd\mathbf{L}_2Cl_2$ was dissolved in DMSO, new dinuclear Pd(II) complexes **4** containing two DMSO molecules in the structure were detected (complex **4** at *m/z*

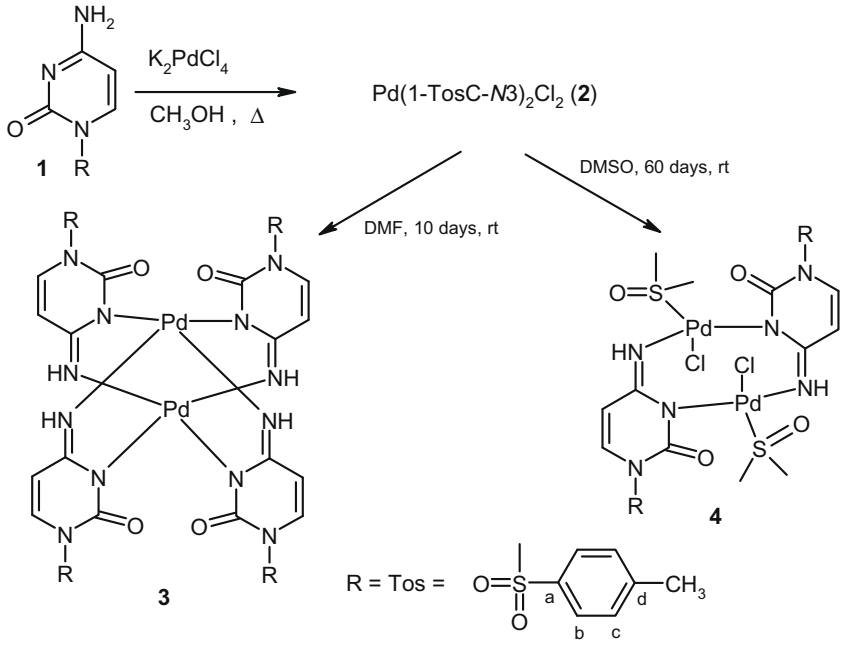

Scheme 2. Synthesis of complexes: Pd(1-TosC–*N*3)$_2$Cl$_2$ (**2**), Pd$_2$(1-TosC$^-$–*N*3,*N*4)$_4$ (**3**) and Pd$_2$(1-TosC$^-$–*N*3,*N*4)$_2$DMSO$_2$Cl$_2$ (**4**).

992.59 assigned as the $[Pd_2(\mathbf{L}–H)_2(DMSO)_2Cl_2Na]^+$ ion or at *m/z* 1009.46 assigned as the $[Pd_2(\mathbf{L}–H)_2(DMSO)_2Cl_2K]^+$ ion, and its fragments). Complex **3** or its fragments were detected by MS at *m/z* 1268.77 assigned as the $[Pd_2(\mathbf{L}–H)_4]^+$ ion or at *m/z* 1290.80 assigned as the $[Pd_2(\mathbf{L}–H)_4]Na^+$ ion or at *m/z* 1308.76 assigned as the $[Pd_2(\mathbf{L}–H)_4]K^+$. A detailed MS study of the complex $Pd\mathbf{L}_2Cl_2$ will be described elsewhere.

3.2.3. Solution studies

Compound **2** is generally insoluble in common organic solvents, except DMF and DMSO. The molar conductivity value in DMSO proves that complex **2** is a non-electrolyte. This finding indicates that both the chloride anions and the organic ligands are located in the internal coordination sphere of the Pd(II) complex. Despite the fact that most palladium complexes (PdL_2Cl_2) exhibit a fast exchange of axial ligands with solvent molecules, **2** is stable in DMSO–d_6 for several days at room temperature.

With respect to the ^{1}H NMR spectrum of ligand **1**, the spectrum (DMSO–d_6) of complex **2** exhibits two pairs of signals for each proton in a 2:1 ratio (Fig. 4). The first set of resonances of **2** (marked o in Fig. 4) displays two sets of doublets in the aromatic region, corresponding to the H-6 and H-5 protons (δ 8.10 and 5.94 ppm) and phenyl Ph-b and Ph-c protons (δ 7.84 and 7.44 ppm). Two amino protons at N-4, readily exchangeable with deuterium by addition of D_2O, appear as a broadened doublet at δ 7.88 ppm. These data are in accord with the keto-amino form of the ligand in the complex Pd(1-TosC–*N*3)$_2$Cl$_2$ (**2**). On the other hand, all the protons of the second set of resonances in the DMSO solution of **2** (marked x in Fig. 4) were shifted upfield. Signals of the H-6 and H-5 (δ 8.22 and 6.07 ppm) and Ph-b and Ph-c protons (δ 7.94 and 7.50 ppm) show significant additional splitting of the H-5, H-6 and Ph doublets and the broadened singlets at δ 9.34, 9.25, 9.21 and 8.89 ppm are assigned to NH protons. The latter observations may be explained by the existence of two possible rotamers in **2**, which is also evident from the infrared spectra.

The ^{1}H NMR spectrum of the dipalladium complex Pd_2(1-TosC$^-$–*N*3,*N*4)$_2$DMSO$_2$Cl$_2$ (**4**) is considerably different and shows only one signal for each H5, H6, Ph-b, Ph-c and NH-4 proton, due to the high symmetry of the complex and large upfield shifts for the H-6 (δ 7.60 ppm, doublet $J_{6,5}$ = 8 Hz) and the NH-4 (δ 7.26 ppm, broad singlet) protons.

Table 2
IR frequencies for cytosine (Cy), ligand **1** and complexes **2** and **4**.

ν (cm^{-1})	Cy	**1**	**2**	**4**
N–H	3387	3369	3406	3407
	3174	3100	3313	3247
			3288	3103
			3247	
			3207	
			3107	
C=O	1664	1703	1686	1670
C=C	1640	1673	1650	1648
C=N	1617	1524	1613	1569
NH_2 ring	1537	1489	1609	1475
	1504		1514	
	1466		1503	
SO_2	–	1376	1380	1396
		1353	1363	1354
		1184	1191	1188
		1173	1171	1172
		1184	1191	1025
		1173	1171	
		1138	1145	
S–N	–	967	974	1018
ν(Pd–N)	–	–	478	490–426
			453	
			417	
ν(Pd–Cl)	–	–	361	370
			305	360
			280	

3.2.4. Infrared spectra

The infrared spectra with tentative band assignments (ν/cm^{-1}) for cytosine, according to the literature [23], some characteristic changes in ligand **1** and the bands in the spectra of complexes **2** and **4** are shown in Table 2. The strong to weak bands, observed between 3407 and 3100 cm^{-1}, are associated with ν(N–H). Ligand **1** (keto-amino tautomer) shows characteristic $\nu_{as}(NH_2)$ and $\nu_s(NH_2)$ vibrations at 3369 and 3100 cm^{-1} for the C4 amino group, while the ketoimino form of the ligand anion in **4** shows the N–H stretching of the imine group at 3407, 3247 and 3103 cm^{-1}, which is also indicated by the ^{1}H NMR spectrum.

Solid $Pd\mathbf{L}_2Cl_2$ (**2**) shows six bands between 3406 and 3107 cm^{-1}, supporting the existence of two rotamers [24]. The band assigned to ν(C(2)=O), which appears around 1703 cm^{-1} in the free ligand spectrum, is appreciably shifted to lower frequencies. This modification and changes in the zone between 1700 and 1400 cm^{-1}, involving the stretching of ν(C=O, C=C, C=N, ring, C–N, etc.), are related to the new charge distribution in the ring of the complexes. For the palladium complex $Pd\mathbf{L}_2Cl_2$ (**2**), three bands at 280, 306 and 360 cm^{-1}, and for complex **4** one split band within 360–370 cm^{-1} are attributed to the ν(Pd–Cl) vibrations, while the bands within the 426–480 cm^{-1} range are assignable to the ν(Pd–N) stretching vibrations [25].

3.2.5. Crystal structure of *3*

The molecular structure of **3** includes two Pd atoms, 2.6210(15) Å apart, with the interatomic Pd1–Pd2 vector along the twofold symmetry axis parallel to the crystallographic *b*-axis. The relatively short interpalladium distance is probably caused by steric hindrance of the bulky ligands. The coordination spheres of both Pd atoms inside the binuclear metal complex are virtually identical. They both consist of two exocyclic imino N4 [Pd1–N4, 1.970(9) Å; Pd2–N4, 2.039(12) Å] and two endocyclic N3 [Pd1–N3, 2.067(10) Å; Pd2–N3, 2.090(9) Å] atoms. The coordination spheres of the two palladium atoms are inseparable since they involve four ligand molecules, each of which binds to one Pd atom through its endocyclic N3 and to the other one through the exocyclic N4; hence each of the four ligand molecules bridges two palladium atoms *via* its N–C–N moiety. The asymmetric unit contains two ligand molecules (**A** and **B**), as well as two Pd atoms with half-site occupancy. The asymmetric unit is then repeated by a twofold symmetry axis operation to give a paddlewheel binuclear structure where the adjacent ligand molecules are head-to-tail oriented with respect to the twofold axis, *i.e.* with respect to the interpalladium vector (Fig. 5).

The complete geometries of both coordination spheres of complex **3** are given in Table 3. The atom numbering in the ligand molecule **B** is composed of a prefix "2" and the second digit, corresponds to the numbering scheme defined for the ligand molecule **A**. Thus, for example, N3 of the ligand molecule **A** corresponds to N23 of the ligand molecule **B**. It is evident that the Pd–N3 (endocyclic nitrogen) contacts are somewhat longer than the Pd–N4 (exocyclic imino-nitrogen) ones. The four nitrogens forming the first coordination sphere around Pd1 (N23, N23*i*, N4 and N4*i*) are in an almost perfect square-planar arrangement. The maximum deviation from the least square plane defined by Pd1 and the four nitrogen atoms is only 0.0891(11) Å, whereas the least square plane defined only by these four nitrogen atoms reveals a maximum deviation of 0.025(11) Å.

Similarly, the Pd2 coordination sphere least square plane including palladium reveals a maximum deviation of 0.0878(9) Å, excluding Pd2, 0.013(11) Å. In addition, remarkable planarity is re-

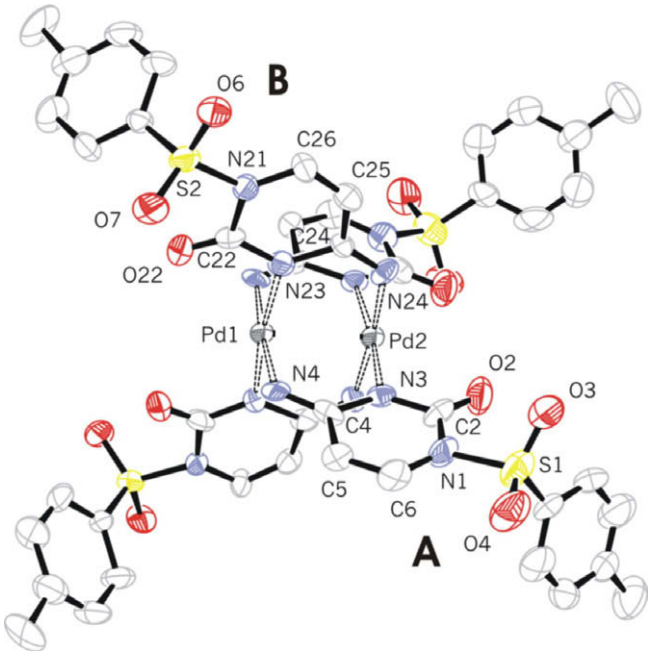

Fig. 5. ORTEP drawing of complex **3** with a partial atom numbering scheme and 30% ellipsoid probability. Hydrogen atoms are omitted for clarity.

vealed by the two planes defined by N3, C4, N4, Pd1, N4*i*, C4*i*, N3*i* and Pd2 [max. deviation of the least square plane, 0.038(10) Å] and N23, C24, N24, Pd1, N24*i*, C24*i*, N23*i* and Pd2 [max. deviation of the least square plane, 0.061(9) Å]. These two planes intersect at the Pd1–Pd2 vector, forming an interplanar angle of 89.3(3)°. This class of ligands reveals a conformational chirality along the N–S bond, as previously described by us [17]. Although **3** crystallizes in the centrosymmetric space group *Pnab*, discrete complex molecules do not contain an intramolecular inversion centre, and all the ligand molecules present inside the single complex molecule are of the same chirality. However, the crystal structure contains complex molecules of both chiralities, related by the extramolecular inversion centers.

The cytosine ring geometries for ligand **1** as well as for complexes **3** and **4** are given in Table 4. In both symmetrically independent ligand molecules **3A** and **3B**, the bond distances inside the cytosine rings reveal remarkable alterations compared to the analogous values in the structure of ligand **1**. This is due to the stabilization of the iminooxo form of the ligand anion upon Pd coordination. While the length of the N3–C4 bond in ligand **1** clearly reflects its double bond character, this bond is significantly longer in both coordinated ligand molecules in complex **3**, suggesting an increase of its single bond character. This implies that the

Table 3
Coordination sphere geometries in **3** (*i*; 1/2 − *x*, *y*, −*z*).

Bond lengths (Å)			
Pd1–N23	2.067(10)	Pd2–N3	2.090(9)
Pd1–N23*i*	2.067(10)	Pd2–N3*i*	2.090(9)
Pd1–N4	1.970(9)	Pd2–N24	2.039(12)
Pd1–N4*i*	1.970(9)	Pd2–N24*i*	2.039(12)
Bond angles (°)			
N23–Pd1–N23*i*	172.4(4)	N3–Pd2–N3*i*	173.3(4)
N23–Pd1–N4	90.9(4)	N3–Pd2–N24	86.3(4)
N23–Pd1–N4*i*	88.8(4)	N3–Pd2–N24*i*	93.4(4)
N23i–Pd1–N4	88.8(4)	N3i–Pd2–N24	93.4(4)
N23i–Pd1–N4*i*	90.9(4)	N3i–Pd2–N24*i*	86.3(4)
N4–Pd1–N4i	175.0(4)	N24–Pd2–N24*i*	174.5(4)

Table 4
Bond distances (Å) inside the cytosine ring in **1**, **3** and **4**.

	1	3A	3B	4A	4B
N1–C2	1.432(3)	1.382(16)	1.504(16)	1.417(12)	1.407(11)
C2–N3	1.339(3)	1.389(16)	1.380(16)	1.334(12)	1.380(12)
N3–C4	1.340(2)	1.421(14)	1.443(14)	1.386(10)	1.374(11)
C4–N4	1.312(3)	1.308(15)	1.279(15)	1.307(12)	1.291(12)
C4–C5	1.436(3)	1.440(15)	1.461(17)	1.429(11)	1.452(12)
C5–C6	1.317(3)	1.351(17)	1.290(15)	1.329(14)	1.308(14)
C6–N1	1.396(3)	1.369(17)	1.381(15)	1.393(13)	1.396(11)

negative charge at the endocyclic N3 atoms compensates the positive charge of the Pd atom in the complex structure.

3.2.6. Crystal structure of *4*

Molecular structure of **4** is given in Fig. 6 as an ORTEP drawing. Complex **4** is a dinuclear bridging molecule where two palladium atoms, being 2.9358(10) Å apart, are each coordinated by one exocyclic imino-nitrogen N4 and one endocyclic nitrogen N3. The coordination spheres are each completed by one DMSO molecule (through its sulfur atom) and one chlorine atom. Two ligand molecules bridge two Pd atoms in such a manner that each ligand complexes one Pd atom with its exocyclic imino-nitrogen N4 and the other one with its endocyclic N3. The positive charge of the Pd atoms (+2) is compensated by one chlorine and one deprotonated endocyclic nitrogen, bearing a negative charge, as a consequence of the iminooxo form stabilization upon Pd complexation (*vide supra*).

The geometry of the cytosine ring is given in Table 4. A comparison with the analogous values observed in the ligand structure reveals an increase of the single bond character of the N3–C4 bond, similarly to the case of complex **3**. In both cases, stabilization of the iminooxo form took place upon the coordination of Pd(II). The two bridging rings involve both palladium atoms, as well as N3, C4 and N4 of both ligand molecules, and the corresponding planes form an interplanar angle of 89.9(2)°. The molecule contains two DMSO molecules coordinated to the Pd atoms through their sulfur atoms. A search of the current version of *CSD* (2007 release) shows that the abundance of O-bonded and S-bonded Pd–DMSO adducts is almost equal. Details of the coordination sphere geometries are given in Table 5. The maximum deviation from the coordination sphere least square plane, defined by Pd1, S3, Cl1, N3 and

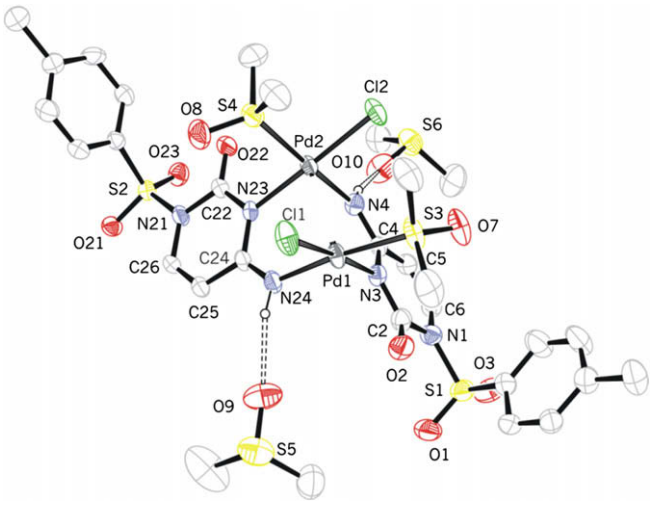

Fig. 6. ORTEP drawing of **4**. Ellipsoids are given on a 30% probability scale. The atom numbering is provided partially and hydrogens are omitted for clarity, except for those included in hydrogen bonding. The solvent molecule connected by the hydrogen bond N24–H···O9 is included.

Table 5
Geometry of the coordination spheres around Pd1 and Pd2 in **4**.

	Pd1	Pd2
Bond lengths (Å)		
Pd–S	2.263(3)	2.252(3)
Pd–Cl	2.292(3)	2.299(2)
Pd–N3 (N23)	2.029(7)	2.034(7)
Pd–N4 (N24)	2.028(8)	2.020(7)
Angles (°)		
S–Pd–Cl	91.10(10)	90.29(10)
S–Pd–N3 (N23)	89.7(2)	89.1(2)
S–Pd–N4 (N24)	173.8(2)	172.5(2)
Cl–Pd–N3 (N23)	176.1(2)	178.5(2)
Cl–Pd–N4 (N24)	90.7(2)	90.3(2)
N3 (N23)–Pd–N4 (N24)	88.1(3)	90.2(3)

N24, is 0.0722(6) Å, whereas in the case of the one defined by Pd2, S4, Cl2, N4 and N23, it is 0.076(7) Å.

The crystal structure is characterized by discrete complex molecules, each of which is connected to two DMSO molecules (in addition to those included in the coordination around Pd), *via* the imino-nitrogens N4 and N24 and the oxygen atoms of the neighbouring non-coordinated solvent molecules [N4–H···O10, 2.965(12) Å, 166°; N24–H···O9, 3.074(15) Å, 146°] (Fig. 6).

4. Conclusions

Complexation of Pd(II) with 1-(*p*-toluenesulfonyl)cytosine ligand (**1**) leads initially to the formation of a kinetically favoured mononuclear complex **2**, regardless of the solvent used. This, initially formed complex undergoes rearrangements in aprotic polar solvents, resulting in the formation of two different dinuclear bridging species (**3** from DMF and **4** from DMSO), where the ligand anion (1-TosC$^-$) exists in a rare iminooxo form and is coordinated to Pd(II) through both its exocyclic (N4) and endocyclic nitrogen atom (N3).

Supplementary data

CCDC 695234, 695235 and 695236 contains the supplementary crystallographic data for compounds **1**, **3** and **4**, respectively. These data can be obtained free of charge via http://www.ccdc.cam.ac.uk/conts/retrieving.html, or from the Cambridge Crystallographic Data Centre, 12 Union Road, Cambridge CB2 1EZ, UK; fax: (+44) 1223-336-033; or e-mail: deposit@ccdc.cam.ac.uk.

Acknowledgments

We thank Dr. sc. Ljerka Tušek-Božić for conductometric measurements. We appreciate the financial support of the Ministry of Science, Education and Sports of the Republic of Croatia through Grants No. 098-0982914-2935, 098-1191344-2943 and 098-0982904-2927.

References

[1] K.A. Hartman, A. Rich, J. Am. Chem. Soc. 87 (1965) 2033.
[2] R.B. Inman, J. Mol. Biol. 9 (1964) 624.
[3] P. Rajagopal, J. Feigon, Nature 339 (1989) 637.
[4] L.C. Sowers, G.V. Fazakerley, R. Eritja, B.E. Kaplan, M.F. Goodman, Proc. Natl. Acad. Sci. USA 83 (1986) 5434.
[5] (a) B. Lippert, H. Schöllhorn, U. Thewalt, J. Am. Chem. Soc. 108 (1986) 6616;
(b) W. Saenger, in: Principles of Nucleic Acid Structure, Springer Verlag, New York, 1982;
(c) M. Monshi, K. Al-Farhan, S. Al-Resayes, G. Ghaith, A.A. Hasanein, Spectrochim. Acta, Part A 53 (1997) 2669.
[6] D. Montagner, E. Zangrando, B. Longato, Inorg. Chim. Acta (2008), doi:10.1016/j.ica.2008.04.030.
[7] (a) F. Zamora, M. Kunsman, M. Sabat, B. Lippert, Inorg. Chem. 36 (1997) 1583;
(b) A.H. Velders, B. van der Geest, H. Kooijman, A.L. Spek, J.G. Haasnoot, J. Reedijk, Eur. J. Inorg. Chem. (2001) 369;
(c) L.Y. Kuo, M.G. Kanatzidis, M. Sabat, A.L. Tipton, T.J. Marks, J. Am. Chem. Soc. 113 (1991) 9027.
[8] P.J.S. Miguel, P. Lax, M. Willermann, B. Lippert, Inorg. Chim. Acta 357 (2004) 4552.
[9] J. Müller, E. Zangrando, N. Pahlke, E. Freisinger, L. Randaccio, B. Lippert, Chem. Eur. J. 4 (1998) 397.
[10] (a) Lj. Glavaš-Obrovac, I. Karner, B. Žinić, K. Pavelić, Anticancer Res. 21 (2001) 1979;
(b) B. Žinić, M. Žinić, I. Krizmanić, EP 0 877 022 B1, Synthesis of the Sulfonylpyrimidine Derivatives with Anticancer Activity, 2003.;
(c) F. Supek, M. Kralj, M. Marjanović, L. Šuman, T. Šmuc, I. Krizmanić, B. Žinić, Invest. New Drugs 26 (2008) 97.
[11] J. Kašnar-Šamprec, Lj. Glavaš-Obrovac, M. Pavlak, I. Mihaljević, V. Mrljak, N. Štambuk, P. Konjevoda, B. Žinić, Croat. Chem. Acta 78 (2005) 261.
[12] L.J. Faruggia, J. Appl. Cryst. 32 (1999) 837.
[13] M.C. Burla, M. Camalli, B. Carrozzini, G.L. Cascarano, C. Giaccovazzo, G. Polidori, R. Spagna, SIR2002, Version 1.0, A Program for Automatic Solution and Refinement of Crystal Structures, University of Bari, Bari, Italy, 2002.
[14] G.M. Sheldrick, SHELX97: Program for the Refinement of Crystal Structures, Universität Göttingen, Germany, 1997.
[15] L.J. Farrugia, J. Appl. Crystallogr. 30 (1997) 565.
[16] P. van der Sluis, A.L. Spek, Acta Crystallogr., Sect. A 46 (1990) 194.
[17] A.L. Spek, PLATON – A Multipurpose Crystallographic Tool, Version 40607, University of Utrecht, Utrecht, The Netherlands, 1998–2007.
[18] A. Višnjevac, M. Žinić, M. Luić, D. Žiher, T. Kajfež Novak, B. Žinić, Tetrahedron 63 (2007) 86.
[19] J. Bernstein, R.E. Davies, L. Shimani, N.-L. Chang, Angew. Chem. 107 (1995) 1689.
[20] J.H. Gross, Mass Spectrometry, Springer, Berlin, 2004.
[21] L.C. Gatlin, F. Tureček, in: R.B. Cole (Ed.), Electrospray Ionization Mass Spectrometry: Fundamentals, Instrumentation, and Applications, Wiley, New York, 1997, p. 527.
[22] M. Franska, Intern. J. Mass Spectrometry 261 (2007) 86.
[23] (a) M. Tsuboi, S. Takahasha, I. Harada, in: J. Duchesene (Ed.), Physicochemical Properties of Nucleic Acids, vol. 2, Academic Press, London, 1973, p. 91;
(b) H. Susi, J.S. Ard, J.M. Purcell, Spectrochim. Acta 29A (1973) 725;
(c) E.D. Radchenko, G.G. Sheina, N.A. Smorygo, Y.P. Blagoi, J. Mol. Struct. 116 (1984) 387;
(d) Y. Nishimura, T. Tsuboi, Chem. Phys. 98 (1985) 71.
[24] E. Nir, I. Huenig, K. Kleinermanns, M.S. de Vries, Phys. Chem. Chem. Phys. 5 (2003) 4780.
[25] (a) L. Szučova, Z. Travniček, M. Zatloukal, I. Popa, Bioorg. Med. Chem. 14 (2006) 479;
(b) I.A. Efimenko, A.P. Kurbakova, Transition Met. Chem. 19 (1994) 539;
(c) P.-C. Kong, F.D. Rochon, Can. J. Chem. 59 (1981) 3293.